Resonance peak shift in the photocurrent of ultrahigh-mobility two-dimensional electron systems

Jesús Iñarrea [1,2]
[1] *Escuela Politécnica Superior, Universidad Carlos III, Leganes, Madrid 28911, Spain*
[2] *Unidad Asociada al Instituto de Ciencia de Materiales, CSIC, Cantoblanco, Madrid 28049, Spain*

(Received 30 October 2019; revised manuscript received 21 February 2020; accepted 6 March 2020; published 18 March 2020)

We report on a theoretical study on the rise of strong peaks at the harmonics of the cyclotron resonance in the irradiated magnetoresistance in ultraclean two-dimensional electron systems. The motivation is the experimental observation of a totally unexpected strong resistance peak showing up at the second harmonic. We extend the radiation-driven electron orbit model (previously developed to study photocurrent oscillations and zero resistance states) to an ultraclean scenario that implies a longer scattering time and longer mean free path. Thus, when the mean free path is equivalent, in terms of energy, to twice the cyclotron energy ($2\hbar w_c$), the electron behaves as under an effective magnetic field that is twice the one actually applied. Then, at high radiation power and/or low temperature, a resistance spike can be observed *at the second harmonic*. For even cleaner samples the energy distance could increase to three or four times the cyclotron energy giving rise to resistance peaks at higher harmonics (third, fourth, etc.), i.e., a resonance peak shift to lower magnetic fields as the quality of the sample increases. Thus, by selecting the sample mobility, one automatically would select the radiation resonance response without altering the radiation frequency.

DOI: 10.1103/PhysRevB.101.115419

Radiation-induced magnetoresistance (R_{xx}) oscillations (MIROs) [1,2] show up in high-mobility two-dimensional electron systems (2DESs) when they are irradiated with microwaves (MWs) at low temperatures ($T \sim 1$ K) and under low magnetic fields (B) perpendicular to the 2DES.

At high enough radiation power (P), maximum and minimum oscillations increase, but the latter evolve into zero resistance states (ZRSs) [1,2]. Both effects were totally unexpected when they were first obtained, revealing some type of different radiation-matter interaction assisting electron magnetotransport [3,4]. Their discovery was considered to be very important, especially in the case of zero resistance states, because they were obtained without quantization in the Hall resistance. Despite the fact that over the last years quite a few important experimental [5–21] and theoretical efforts [22–36] have been made on MIROs and ZRSs, their physical origin still remains unclear and controversial.

Resonance phenomena can be found widely in nature and occur with all types of oscillations, from sound to electromagnetic radiation. They are extremely interesting in physics, from theoretical to application perspectives, because they give rise to an intense energy transfer between an exciting source and a driven system. But it turns out definitively more intriguing and puzzling when the resonance takes place off the natural oscillation frequency. This applies to one of the most challenging experimental findings [37,38] regarding MIROs and as unexpected as ZRSs. It consists of a prominent resistance peak that shows up at the second harmonic of the cyclotron frequency $w \simeq 2w_c$ (w is the radiation frequency and w_c the cyclotron frequency) in irradiated R_{xx} [37,38] of ultrahigh-mobility 2DES. This extremely high mobility ($\mu \geqslant 3 \times 10^7$ cm^2/V s) along with a low T and high P play an essential role in the appearance of this striking result. The amplitude of such a spike is very large regarding the usual MIRO, suggesting a resonance effect but off the expected position, $w \simeq w_c$. To date, very few theoretical models have been presented on this topic [39,40].

In this article, we present a theoretical analysis of this resonance peak shift based on the radiation-driven electron orbit model [22,23] but adapted to a scenario of ultrahigh-quality samples (reduced electron scattering). In the extension of the model we start considering that these kinds of samples have increasingly longer mean free paths and scattering times. Thus, the scattered electron that jumps between Landau orbits (Landau states) can reach much further, in distance and energy, the final Landau orbits (due to the DC electric field applied in the x direction; see Fig. 1), for instance, orbits located at twice the cyclotron energy ($2\hbar w_c$). For this specific case the electron would behave, from the scattering standpoint, as under an *effective* magnetic field of double intensity than the one actually applied. Then, the spike will rise, at low enough T and high enough P, at the second harmonic. For even higher mobilities we would still have longer mean free paths and then we can predict the subsequent rise of R_{xx} spikes at higher harmonics: $3w_c = w$, $4w_c = w$, $5w_c = w$, etc., i.e., at lower and lower B. Therefore, and as a main result, we conclude that by controlling the mobility of 2DES we can shift the resonance response without altering the radiation frequency. This result could turn out to be very interesting for device engineering and applications. For instance, by irradiating a ultraclean 2D sample with terahertz radiation we would obtain a resonance response in a B region corresponding to MW or even lower frequencies.

Another important result from our theoretical model is that both MIRO and R_{xx} spikes would share the same physical origin. Thus, they would stem from the interplay of the

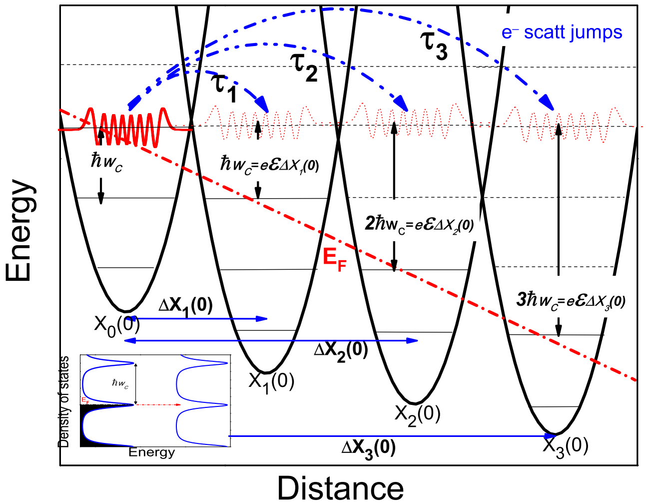

FIG. 1. Schematic diagram describing elastic scattering between tilted Landau orbits (Landau states) according to $n\hbar w_c = e\xi\,\Delta X_n(0)$. ξ is the DC driving electric field and $X_n(0)$ are the positions of the corresponding Landau orbits. The maximum contribution to the current is obtained when the Landau levels involved in the scattering jumps are aligned (see inset).

radiation-driven swinging motion of the irradiated Landau orbits and the scattering of electrons with charged impurities. Thus, the large R_{xx} spike would correspond to a resonance effect between the frequency of the Landau orbit harmonic motion and w_c. Obviously, the former turns out to be the same as radiation frequency.

The *radiation-driven electron orbit model* was devised by the authors to address two physical effects triggered by radiation: MIRO and ZRS in a high-mobility 2DES. According to this model, under radiation, the Landau orbits spatially and harmonically oscillate with the radiation frequency. As a result, the scattering process of electrons with charged impurities turns out to be dramatically altered. This is reflected in magnetotransport and in turn in R_{xx} giving rise to the well-known MIRO and ZRS [22,23,41–43]. Following the model, we use a semiclassical Boltzmann theory to calculate the longitudinal conductivity σ_{xx} [44–46],

$$\sigma_{xx} = 2e^2 \int_0^\infty dE\, \rho_i(E)(\Delta X)^2 W_I \left(-\frac{df(E)}{dE}\right), \qquad (1)$$

with E the energy and $\rho_i(E)$ the density of the initial Landau states. The expression for ΔX is likewise obtained from the model [47,48]

$$\Delta X = \Delta X_1(0) - A(w_c)\sin(w\tau_1), \qquad (2)$$

where $\Delta X_1(0)$ is the distance between the guiding centers of the final and initial Landau orbits in the dark and $\tau_1 = 2\pi/w_c$ is the *flight time*, the time it takes the scattered electron between Landau orbits. It was previously proposed, in a semiclassical approach [47,49], that during the scattering jump electrons in their orbits would complete, on average, an integer number of cyclotron orbits, which implies that $\tau_n = nT_c = n\frac{2\pi}{w_c}$, with T_c being the cyclotron time. Therefore, the electron involved in the scattering ends up in the same relative position inside the final orbit as the one it started from in the initial one. The reason for this is that the dynamics of the orbits (Landau states) is governed on average by the position of the center of the orbit irrespective of the electron position inside the orbit when the scattering takes place. Then, on average, both the initial and final semiclassical positions are identical in their respective orbits. In the radiation-driven electron orbit model [47,48], $n = 1$ and $\tau_1 = T_c$ correspond to one cyclotron orbit during the jump. $A(w_c)$ is the amplitude of the spatial oscillations of the driven orbits in the x direction,

$$A(w_c) = \frac{eE_0 \sin wt}{m^* \sqrt{\left[w_c^2 - w^2\right]^2 + \gamma^4}}, \qquad (3)$$

with E_0 the radiation electric field and γ is a damping parameter related to the interaction of the electrons in the driven Landau orbits with the lattice ions. W_I is the scattering rate of electrons with charged impurities that, according to the Fermi's golden rule, $W_I = \frac{2\pi}{\hbar}|\langle\phi_f|V_s|\phi_i\rangle|^2\delta(E_i - E_f)$, where ϕ_i and ϕ_f are the wave functions corresponding to the initial and final Landau states, respectively, and V_s is the scattering potential for charged impurities [45]. The expressions of the initial and final energies are $E_i = \hbar w_c(i + 1/2)$ and $E_f = \hbar w_c(f + 1/2) - \Delta_{\rm DC}$, where i and f are integers, and $\Delta_{\rm DC} = e\xi\,\Delta X(0)$, where ξ is the DC driving electric field in the x direction and responsible of the current along that direction (see Fig. 1). To obtain R_{xx} we use the common tensorial relation $R_{xx} = \frac{\sigma_{xx}}{\sigma_{xx}^2+\sigma_{xy}^2} \simeq \frac{\sigma_{xx}}{\sigma_{xy}^2}$, where $\sigma_{xy} \simeq \frac{n_i e}{B}$, with n_i being the electron density, e the electron charge, and $\sigma_{xx} \ll \sigma_{xy}$.

According to W_I, the largest contributions to the conductivity in the presence of the field ξ occur when $E_i = E_f \Rightarrow e\xi\,\Delta X_n(0) \simeq n\hbar w_c$, implying that the Landau level indices f and i are related by $f = i + n$, with n being a positive integer, or in other words, when the Landau levels are aligned (see the inset in Fig. 1). The $n = 1$ scenario labeled with τ_1 in Fig. 1 implies that $e\xi\,\Delta X_1(0) = \hbar w_c$ and it would correspond to ordinary MIRO. In a general extension of the model we can include other scattering processes that are likewise likely to happen according to W_I (their Landau levels are aligned, too). These processes are labeled in Fig. 1, with τ_2 and τ_3 (flight times of theses processes) corresponding to energy differences (in reference to the Fermi energy) of $e\xi\,\Delta X_2(0) = 2\hbar w_c$ and $e\xi\,\Delta X_3(0) = 3\hbar w_c$, respectively (see Fig. 1). Yet, the long distance between the Landau orbits involved in the scattering (longer than the mean free path in ordinary samples) prevents them from happening; the corresponding probability is very small. Accordingly, and in light of the uncertainty principle [50], the minimum values of those flight times can be obtained: $\tau_2 = 2\pi/2w_c$ and $\tau_3 = 2\pi/3w_c$, respectively. Thus, we obtain increasingly shorter flight times in increasingly longer mean free paths.

Interestingly enough and according to the above, the process labeled with τ_2 would be mainly described by scattering quantities such as the distance between Landau orbits $\Delta X_2(0)$ (scattering mean free path) and the corresponding flight time, both given by

$$e\xi\,\Delta X_2(0) = \hbar w_{c_{\rm eff}}, \qquad (4)$$

$$\tau_2 = \frac{2\pi}{w_{c_{\rm eff}}}, \qquad (5)$$

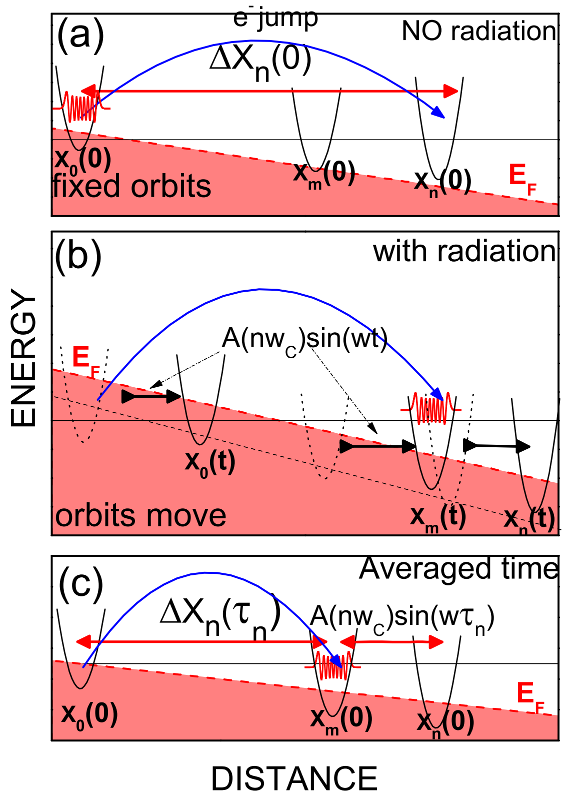

FIG. 2. Schematic diagrams for the emergence of a valley in MIRO in an extended scenario (distant Landau orbits). (a) Elastic scattering (charged impurities) between Landau orbits without radiation. (b) Elastic scattering with radiation where all Landau orbits oscillate at radiation frequency. The $X_n(0)$ position is now occupied by a driven Landau orbit $X_m(0)$, where the scattered electron lands in a time $t = \tau_n$. (c) With radiation but in the steady state after time average. The final averaged distance is smaller than in the dark, giving rise to a MIRO valley. Similar reasoning can be applied for a MIRO peak.

where

$$\hbar w_{c_{\rm eff}} = \hbar \frac{eB_{\rm eff}}{m^*} = \hbar \frac{e(2B)}{m^*} = 2\hbar w_c. \tag{6}$$

Then, the scattered electron reaches the same Landau orbits with the same mean free path and flight time as with a double magnetic field. Then we would obtain scattering results as if the electron were under an effective, twice as high magnetic field ($B_{\rm eff}$) than the one actually applied (B). A similar approach can be applied to the τ_3 and further scenarios. Thus, for τ_3 we would have an effective magnetic field $B_{\rm eff} = 3B$ and $w_{c_{\rm eff}} = 3w_c$. Therefore in our model the increasing quality of the sample makes the main scattering quantities vary in the same way as an increasing magnetic field would. The above discussion is essential for the model and would be at the heart of the experimental results as we explain below. Now, applying the theory of a radiation-driven electron orbit model [48] to these scenarios (from τ_1 to τ_2 and τ_3, etc.), we obtain a general expression for ΔX,

$$\begin{aligned}\Delta X = &[\Delta X_1(0) - A(w_c)\sin(w\tau_1)] \\ &+ [\Delta X_2(0) - A(2w_c)\sin(w\tau_2)] \\ &+ [\Delta X_3(0) - A(3w_c)\sin(w\tau_3)] + \cdots ,\end{aligned} \tag{7}$$

where

$$A(2w_c) = \frac{eE_0 \sin wt}{m^* \sqrt{[(2w_c)^2 - w^2]^2 + \gamma^4}} \tag{8}$$

and

$$A(3w_c) = \frac{eE_0 \sin wt}{m^* \sqrt{[(3w_c)^2 - w^2]^2] + \gamma^4}}. \tag{9}$$

Accordingly, we could obtain the resonance peak in different B positions depending on what is the predominant term over the rest. In the general expression above, we have extended the basic idea of our model that when the radiation is on, the Landau orbits oscillate (driven by radiation), altering the electron scattering. For different flight times (depending of the scenario) $\tau_n = 2\pi/nw_c$, the scattered electron will be *landing* in a different final Landau orbit and will be different in turn from the dark, giving rise to a distance shift in the scattering jump. After averaging out, the shift is given by $A(nw_c)\sin(w\tau_n)$ (see Fig. 2). This shift can be positive or negative (or zero) and is finally reflected in σ_{xx} and R_{xx} in the form of peaks and valleys, respectively, i.e., photoexcited R_{xx} oscillations or MIRO.

As we said above, in an ordinary MIRO experiment only the expression of the first bracket in the right part of the latter equation (the $[\Delta X_1(0) - A(w_c)\sin(w\tau_1)]$ term) would significantly contribute to ΔX. In this regime the shorter mean free path prevents one from reaching further Landau orbits,

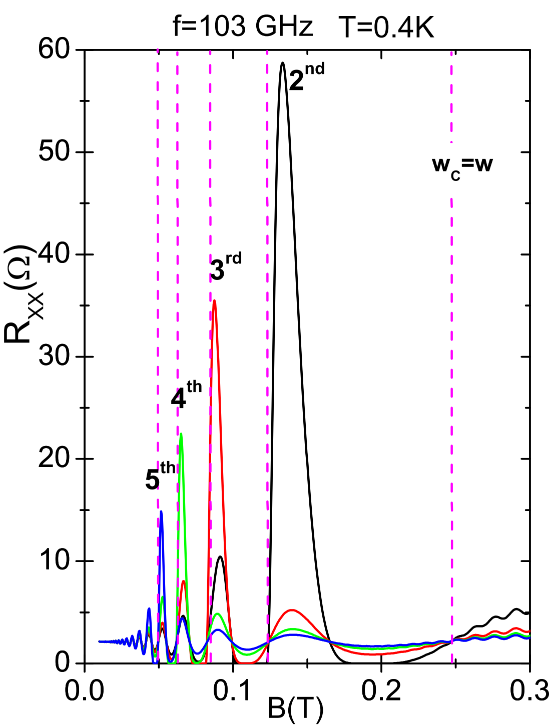

FIG. 3. Calculated magnetoresistance vs B under radiation of 103 GHz and $T = 0.4$ K for four resonance regimes: $2w_c = w$, $3w_c = w$, $4w_c = w$, and $5w_c = w$. Vertical dashed lines mark the harmonic positions. Spikes rise up from the second to fifth harmonic. The photoexcited oscillation positions remain constant showing a 1/4 cycle phase shift independently of the resonance peak displacement.

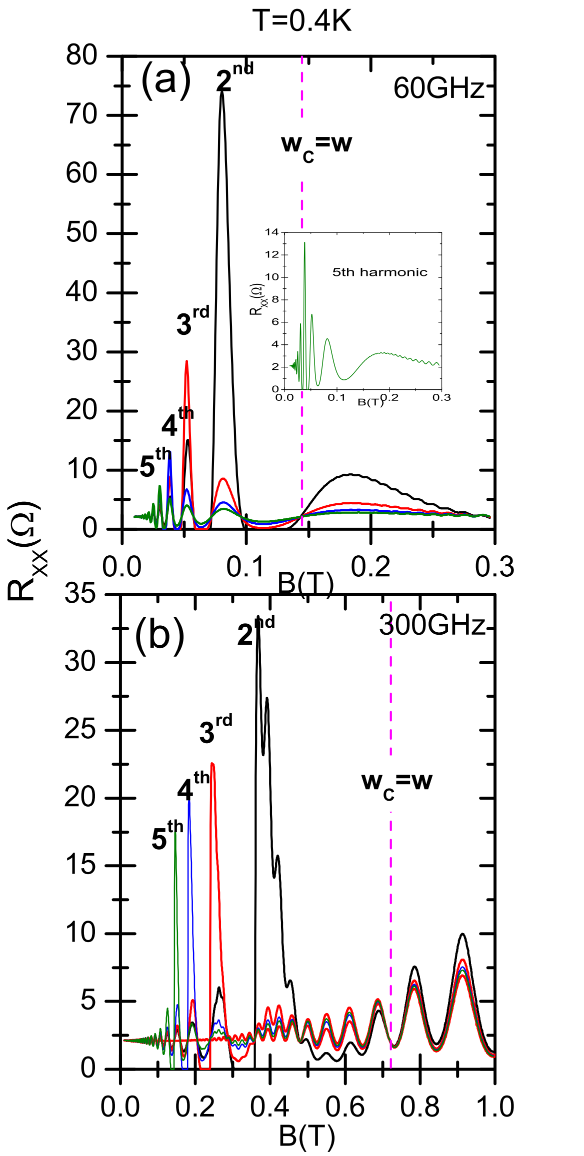

FIG. 4. Same as in Fig. 3. We exhibit the same four off-resonance spikes for 60 GHz in (a) and for 300 GHz in (b). The vertical dashed line for both panels corresponds to the main resonance frequency. The inset in (a) is a zoom-in of the fifth harmonic.

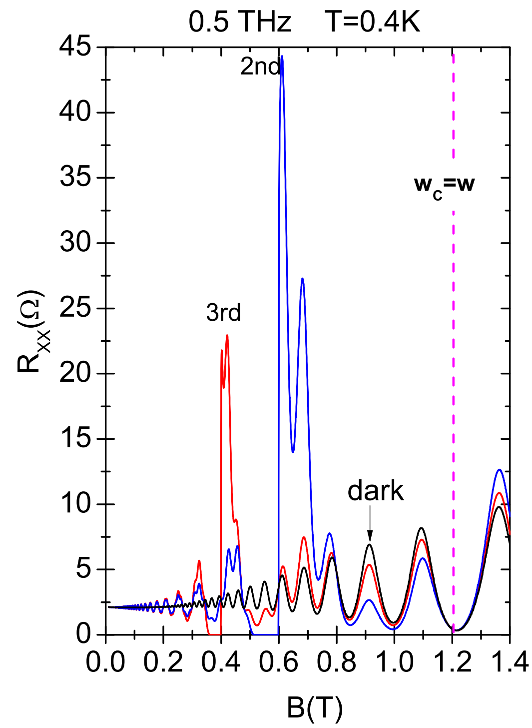

FIG. 5. Same as in Fig. 3 for a frequency of 0.5 THz. We exhibit two off-resonance spikes for the second and third harmonic positions. The vertical dashed line corresponds to the main resonance frequency.

making the contributions of the other terms negligible. Nevertheless, when it comes to ultrahigh-mobility samples we will have longer mean free paths and scattering times, and much further final Landau orbits can be accessible via scattering. Thus, by increasing mobility we would end up having first the $[\Delta X_2(0) - A(2w_c)\sin(w\tau_2)]$ term as predominant where the resonance peak would rise at the second harmonic. In a next step, by further increasing the mobility, even more distant Landau orbits would be accessible and thus we would obtain the third term ($[\Delta X_3(0) - A(3w_c)\sin(w\tau_3)]$) as predominant and the resonance at the third harmonic, etc. For instance, what it is obtained in the off-resonance experiments [37,38] would be based on the second term and the expression of the average advanced distance would be $\Delta X \simeq [\Delta X_2(0) - A(2w_c)\sin(w\tau_2)]$. However, the flight time τ_2 still needs to be adapted to an ultraclean scenario, i.e., it has to be increased as the scattering time increases, too. As we said above in our model, this increment has to be made in multiples of T_c corresponding to the effective magnetic field. This implies that now $\tau_2 = 2 \times 2\pi/2w_c$. Substituting in ΔX, we finally obtain $\Delta X \simeq [\Delta X_2(0) - A(2w_c)\sin(2\pi\frac{w}{w_c})]$. The latter is a remarkable result because it can be generalized to higher-order terms where, as the magnetoresistance resonance peak shifts to lower B, the photoexcited oscillations (MIROs) would remain at the same B position. This is in agreement with experiments [37,38].

In Fig. 3 we exhibit the calculated magnetoresistance versus B under a radiation of 103 GHz and $T = 0.4$ K. We present four curves, each one corresponding to a different resonance regime: $2w_c = w$, $3w_c = w$, $4w_c = w$, and $5w_c = w$. Spikes are obtained from the second to fifth harmonic. The harmonic positions are given by the dashed vertical lines (including the main resonance). As explained above, the oscillation positions remain constant, showing a 1/4 phase shift independently of the resonance peak displacement that moves to lower B for each harmonic. In Fig. 4 we present similar results to Fig. 3 but for two distant frequencies of the microwave band to prove that the off-resonance spikes are a generic feature of MIRO. However, they can only be observed clearly with ultraclean 2DES, cleaner that the ordinary conditions to observe MIRO and ZRS. We exhibit the four off-resonance spikes for 60 GHz in Fig. 4(a) and for 300 GHz in Fig. 4(b). The vertical dashed line for both panels corresponds to the main resonance frequency. In Fig. 5 we exhibit calculated results corresponding to the terahertz band for a radiation frequency of 0.5 THz. Thus, we present the same as in Fig. 3 but for only two irradiated curves corresponding to the $2w_c = w$ and $3w_c = w$ resonance regimes. Thus, on the one hand, we want to demonstrate that this effect can show up at higher frequencies than the microwave band, proving that it can be considered as a universal effect. On the other hand, from the application standpoint it might be interesting to stress that for a terahertz frequency we can obtained the resonance response clearly inside the microwave range just by increasing the mobility of the sample.

In summary, we have presented a theoretical approach on off-resonance spike generation in irradiated magnetoresistance in ultraclean 2DES. We have explained the experiments where the spike at the second harmonic is obtained and predict the appearance of subsequent spikes at higher harmonics for higher mobilities. We have explained this striking effect from the perspective of the radiation-driven electron orbit model based on the idea that these kinds of samples have a longer mean free path. Thus, when, in terms of energy, this distance is twice the cyclotron energy, the electron behaves as under an effective B that is double the one actually applied. Then, a resistance spike *at the second harmonic* can be observed.

This work is supported by the MINECO (Spain) under Grant No. MAT2017-86717-P, ITN Grant No. 234970 (EU), and Grupo de Matematicas Aplicadas a la Materia Condensada (UC3M), Unidad Asociada al CSIC.

[1] R. G. Mani, J. H. Smet, K. von Klitzing, V. Narayanamurti, W. B. Johnson, and V. Umansky, Nature (London) **420**, 646 (2002).
[2] M. A. Zudov, R. R. Du, L. N. Pfeiffer, and K. W. West, Phys. Rev. Lett. **90**, 046807 (2003).
[3] J. Iñarrea and G. Platero, Phys. Status Solidi A **203**, 1148 (2006).
[4] J. Iñarrea, R. Aguado, and G. Platero, Europhys. Lett. **40**, 417 (1997).
[5] R. G. Mani, J. H. Smet, K. von Klitzing, V. Narayanamurti, W. B. Johnson, and V. Umansky, Phys. Rev. Lett. **92**, 146801 (2004).
[6] R. G. Mani, J. H. Smet, K. von Klitzing, V. Narayanamurti, W. B. Johnson, and V. Umansky, Phys. Rev. B **69**, 193304 (2004).
[7] R. L. Willett, L. N. Pfeiffer, and K. W. West, Phys. Rev. Lett. **93**, 026804 (2004).
[8] R. G. Mani, Physica E (Amsterdam) **22**, 1 (2004).
[9] J. H. Smet, B. Gorshunov, C. Jiang, L. Pfeiffer, K. West, V. Umansky, M. Dressel, R. Meisels, F. Kuchar, and K. von Klitzing, Phys. Rev. Lett. **95**, 116804 (2005).
[10] Z. Q. Yuan, C. L. Yang, R. R. Du, L. N. Pfeiffer, and K. W. West, Phys. Rev. B **74**, 075313 (2006).
[11] R. G. Mani, W. B. Johnson, V. Umansky, V. Narayanamurti, and K. Ploog, Phys. Rev. B **79**, 205320 (2009).
[12] S. Wiedmann, G. M. Gusev, O. E. Raichev, A. K. Bakarov, and J. C. Portal, Phys. Rev. Lett. **105**, 026804 (2010).
[13] S. Wiedmann, G. M. Gusev, O. E. Raichev, A. K. Bakarov, and J. C. Portal, Phys. Rev. B **81**, 085311 (2010).
[14] D. Konstantinov and K. Kono, Phys. Rev. Lett. **103**, 266808 (2009).
[15] S. I. Dorozhkin, L. Pfeiffer, K. West, K. von Klitzing, J. H. Smet, Nat. Phys. **7**, 336 (2011).
[16] R. G. Mani, C. Gerl, S. Schmult, W. Wegscheider, and V. Umansky, Phys. Rev. B **81**, 125320 (2010).
[17] R. G. Mani, A. N. Ramanayaka, and W. Wegscheider, Phys. Rev. B **84**, 085308 (2011).
[18] J. Inarrea, R. G. Mani, and W. Wegscheider, Phys. Rev. B **82**, 205321 (2010).
[19] R. G. Mani, Int. J. Mod. Phys. B **18**, 3473 (2004); Physica E **25**, 189 (2004).
[20] T. Ye, H.-C. Liu, W. Wegscheider, and R. G. Mani, Phys. Rev. B **89**, 155307 (2014).
[21] T. Y. Ye, H. C. Liu, Z. Wang, W . Wegscheider, and R. G. Mani, Sci. Rep. **5**, 14880 (2015).
[22] J. Iñarrea and G. Platero, Phys. Rev. Lett. **94**, 016806 (2005).
[23] J. Iñarrea and G. Platero, Phys. Rev. B **72**, 193414 (2005).
[24] J. Iñarrea, Appl. Phys. Lett. **100**, 242103 (2012).
[25] J. Inarrea and G. Platero, Phys. Rev. B **84**, 075313 (2011).
[26] J. Iñarrea, Appl. Phys. Lett. **99**, 232115 (2011).
[27] A. C. Durst, S. Sachdev, N. Read, and S. M. Girvin, Phys. Rev. Lett. **91**, 086803 (2003).
[28] X. L. Lei and S. Y. Liu, Phys. Rev. Lett. **91**, 226805 (2003).
[29] V. Ryzhii *et al.*, Sov. Phys. Semicond. **20**, 1299 (1986).
[30] P. H. Rivera and P. A. Schulz, Phys. Rev. B **70**, 075314 (2004).
[31] J. Iñarrea and G. Platero, Phys. Rev. B **78**, 193310 (2008).
[32] J. Iñarrea, Appl. Phys. Lett. **92**, 192113 (2008).
[33] J. Inarrea and G. Platero, Appl. Phys. Lett. **95**, 162106 (2009).
[34] J. Iñarrea, Appl. Phys. Lett. **90**, 262101 (2007).
[35] J. Inarrea, C. Lopez-Monis, A. H. MacDonald, and G. Platero, Appl. Phys. Lett. **91**, 252112 (2007).
[36] J. Inarrea, J. Appl. Phys. **113**, 183717 (2013).
[37] Y. Dai, R. R. Du, L. N. Pfeiffer, and K. W. West, Phys. Rev. Lett. **105**, 246802 (2010).
[38] A. T. Hatke, M. A. Zudov, L. N. Pfeiffer, and K. W. West, Phys. Rev. B **83**, 121301(R) (2011).
[39] J. Inarrea, Phys. Status Solidi RRL **6**, 394 (2012).
[40] V. A. Volkov and A. A. Zabolotnykh, Phys. Rev. B **89**, 121410(R) (2014).
[41] J. Inarrea and G. Platero, Appl. Phys. Lett. **89**, 172114 (2006).
[42] E. H. Kerner, Can. J. Phys. **36**, 371 (1958).
[43] K. Park, Phys. Rev. B **69**, 201301(R) (2004).
[44] B. K. Ridley, *Quantum Processes in Semiconductors*, 4th ed. (Oxford University Press, Oxford, U.K., 1993).
[45] T. Ando, A. Fowler, and F. Stern, Rev. Mod. Phys. **54** 437 (1982).
[46] N. Miura, *Physics of Semiconductors in High Magnetic Fields* (Oxford University Press, Oxford, U.K., 2008).
[47] J. Inarrea and G. Platero, J. Phys.: Condens. Matter **27**, 415801 (2015).
[48] J. Inarrea, Sci. Rep. **7**, 13573 (2017).
[49] P. E. Brito and H. N. Nazareno, Eur. J. Phys. **28**, 9 (2007).
[50] C. Cohen-Tannoudji, B. Diu, and F. Laloe, *Quantum Mechanics* (Wiley, New York, 1977).